DAMAGE CHARACTERISTICS AND RESIDUAL COMPRESSIVE STRENGTH OF COMPOSITE HONEYCOMB SANDWICH PANELS

G. Zhou and M. Hill, G.Zhou@Lboro.ac.uk, Dept. of Aeronautical & Automotive Engineering, Loughborough University, Loughborough, Leicestershire LE11 3TU, UK

Keywords: *honeycomb, sandwich panel, impact damage, energy absorption, compression-after-impact, damage tolerance*

Abstract

An experimental study of the in-plane compressive behaviour of both aluminium and nomex composite sandwich panels with 8 ply carbon/epoxy skins is conducted. All sandwich panels were impact-damaged at impact energy ranging from 2 J to 55 J. Dominant damage mechanisms were found to be core crushing, skin delamination and fracture with the former two absorbing most impact energy. While undamaged panels failed in region close to one loaded end, all impact-damaged nomex panels failed around the mid-section region. Two thirds of aluminium panels also failed in the mid-section region and one third failed in the loaded end region. The presence of the core played a unique role in in-plane compression and counteracted the deleterious effect of impact damage. The in-plane compressive behaviour has shown combined effects of impact damage and the core in a complex manner.

1 Introduction

Composite sandwich constructions are widely used in aerospace structures due to their light weight, high specific bending stiffness and strength under distributed loads, very good buckling resistance and good energy-absorbing capacity.

A major concern with these sandwich structures is their susceptibility to localised impact damage, which could be caused by tool dropping, hail stones, or runway debris. As a result, a multitude of damage mechanisms such as skin delamination and fracture, skin-core debonding, core crushing and shear failure could occur. To maintain the aforementioned advantages in any of these impact events, both mechanical properties from skins (e.g. interlaminar shear and compressive strengths) and core (e.g. density) and geometric properties (e.g. skin thickness) must be tailored in a design analysis for sandwich structures to be damage tolerant. This requires a thorough understanding of damage and its energy-absorbing characteristics associated with impact event, damage resistance and damage tolerance of sandwich structures.

A great of deal of research has been conducted to examine impact damage and residual compressive strength in sandwich structures [1]. However, in evaluating the effect of impact damage on the residual compressive strength, most research adopted either simple bending approach or column compression approach. A very limited knowledge is available on compression-after-impact (CAI) approach, in which unloaded edges of impact-damaged sandwich panels are simply supported upon in-plane compression [1-8]. The latter, evolved from the impact damage tolerance philosophy for monolithic panels, is employed in current work.

In early reports [8-9] of current investigation, damage mechanisms induced in both aluminium and nomex honeycomb sandwich panels were identified; the effects of skin thickness, core density and material, indenter nose shape, panel diameter and support condition on the damage characteristics were studied; The energy-absorbing characteristics of identified damage mechanisms were examined. The present work reports results of a systematic investigation into the in-plane compressive behaviour of both intact and impact-damaged composite honeycomb sandwich panels.

2 Sandwich Materials and Panel Manufacture

Composite skins were made of unidirectional carbon/epoxy T700/LTM45-EL prepreg with a ply thickness of 0.128 mm. A symmetric cross-ply lay-up of $(0/90)_{2s}$ was selected due primarily to strength considerations. Although various skin thicknesses have been made, only the 8 ply skins were used in fabricating in-plane compression panels. Two types of honeycomb cores used are 5052 aluminium with a density of 70 kg/m^3 (4.4-3/16-15) and nomex with a

density of 64 kg/m^3 (HRH-3/16-4.0). The core depth of both aluminium and nomex honeycombs was 12.7 mm and a nominal panel thickness was 14.7 mm. The nomex honeycomb was dried in an oven overnight at 65^{0}C before being bonded to the skins to remove any moisture absorbed from the atmosphere. Adhesive VTA260 was selected for interfacial bonding.

Skin laminates of 300 × 200 mm were laid up and cured first in an autoclave at 60°C under a pressure of 0.62 MPa (90 psi) for 18 hours. To aid adhesion, the skins were degreased before bonding. The 0° direction of the carbon fibres within the skins was aligned with the ribbon direction of the honeycomb core. For aluminium panels, each skin was separately bonded to the core in an oven at 80°C for 5 hours under a pressure of 0.1 MPa (15 psi). For nomex panels, skins were bonded to the core in an autoclave under the same conditions. Because of the condensation of nomex cells (a couple of cells around the panel edges), the pieces of nomex core used were slightly larger than that of the skins so that the condensed cells could be trimmed off. The sandwich panel was then cut into two nominal 200 mm x 150 mm specimens with the longer side aligned with the direction of compressive loading. Back-to-back strain gauges were bonded on the panel surfaces at selected locations in both the longitudinal and transverse directions (shown in Fig. 2(a)) to monitor mean (or membrane) and panel bending strains. These strain data allowed both the local and global behaviour of the panels to be examined.

3 Experimental Procedures

3.1 Drop-weight low-velocity impact tests

Impact tests were carried out on a purpose-built instrumented drop-weight impact rig in Fig. 1(a) by using a hemispherical (HS) impactor of 20 mm diameter with a 1.5 kg mass. Impact energies were regulated by selecting desired drop heights and ranged from 2 J to 55 J in this investigation. Each rectangular carbon/epoxy plate of 200 mm by 150 mm with a circular testing area of 100 mm in diameter was clamped by using a clamping device, as illustrated in Fig. 1(b). Both impact and rebound velocities were measured respectively by two counters recording times over the distance fixed by a pair of photodiodes. This allows absorbed energies to be calculated directly. For high impact energies, rebound velocities could be slightly underestimated due to the panel deflections thereby overestimating absorbed energies. Both impact force and strain gauge responses could be recorded by a Microlink 4000 data acquisition system with a sampling rate of 50 μs. At each selected impact energy level, three impact tests were conducted with one being diametrically cut up for examination of damage mechanisms and the remaining two being reserved for in-plane compression test. The absorbed energy was also calculated via the closed area under load-displacement curves. All impact test results along with the extents of crushed core and skin delaminations are summarised in Table 1.

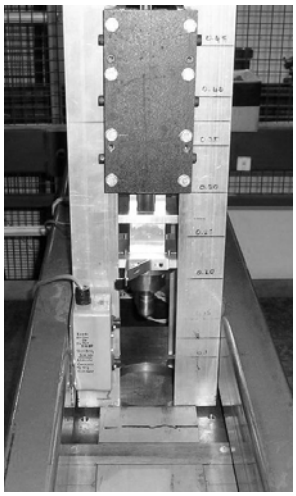

Fig. 1(a) Instrumented drop-weight impact test rig

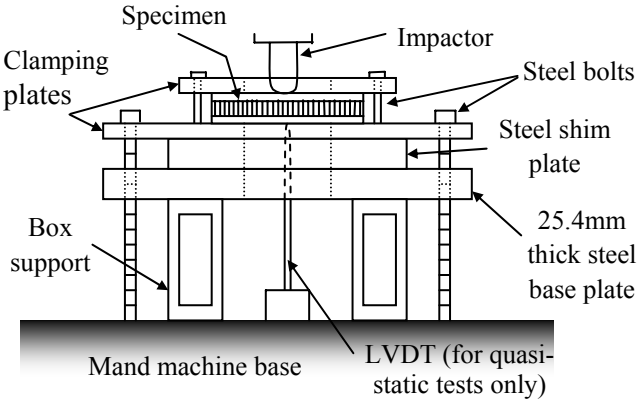

Fig. 1(b) Experimental set-up of a clamped for panel bending test

Table 1 Summary of impact tests

Panel ID	IKE	Absorbed energy	% absorption	Delam. extent	Core damage extent
-	J	J	-	mm	mm
Al control 1	0	0	0	0	0
Al control 2	0	0	0	0	0
Al 3.7J 1	2.60	1.75	0.67	-	-
Al 3.7J 2	3.66	2.44	0.67	30	32
Al 3.7J 3	3.62	2.39	0.65	30	32
Al 5J 1	5.20	3.49	0.67	42	39
Al 5J 2	5.40	3.55	0.66	42	39
Al 9.5J 1	9.54	6.11	0.64	-	-
Al 9.5J 2	9.51	6.60	0.69	-	-
Al 13J 1	13.68	9.19	0.67	53	57
Al 13J 2	13.76	9.22	0.67	53	57
Al 25J 1	24.34	24.24	1.00	66	74
Al 25J 2	25.54	24.15	0.95	66	74
Nom con. 1	0	0	0	0	0
Nom con. 2	0	0	0	0	0
Nom 5J	5.13	2.83	0.55	35	33
Nom 9J	9.23	5.45	0.59	44	49
Nom 16J	16.29	10.03	0.62	59	64
Nom 28J	28.20	26.54	0.94	66	101

3.2 In-Plane Compression Test

As part of the compression specimen preparation, the core at the panel ends intended for applying compressive load was removed to a depth of about 5 mm (slightly more than one cell size). Epoxy end pots were cast between the two skins to prevent an end-brooming failure and the two potted ends were machined to parallel. In each in-plane compression test (popularly known as compression-after-impact (CAI) test), a panel was placed in a purpose-built support jig, as illustrated in Fig. 2(b). The jig provides simple support along the unloaded edges, which were free to move in the width direction during loading. Quasi-static load was applied to the panel at the machined ends via either a Denison or Mand universal testing machine at less than 1 mm/ min.. Although the loaded ends were not clamped, they were effectively close to the clamped condition but without clamping surface pressure. Load, strain and cross-head displacement in all tests were recorded through the same data acquisition system at a sampling rate of 0.5 Hz. All tested panels were cut up for study of damage mechanisms. All in-plane compression results for both intact and impact-damaged panels are summarised in Table 2. To aid understanding of the in-plane compressive behaviour of sandwich panels, a small number of 16 ply monolithic cross-ply panels had also been compression tested.

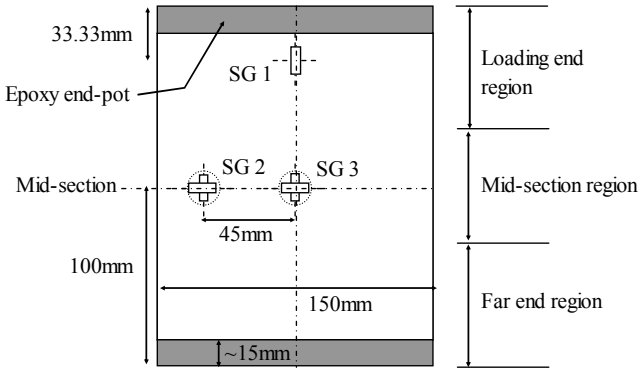

(a)

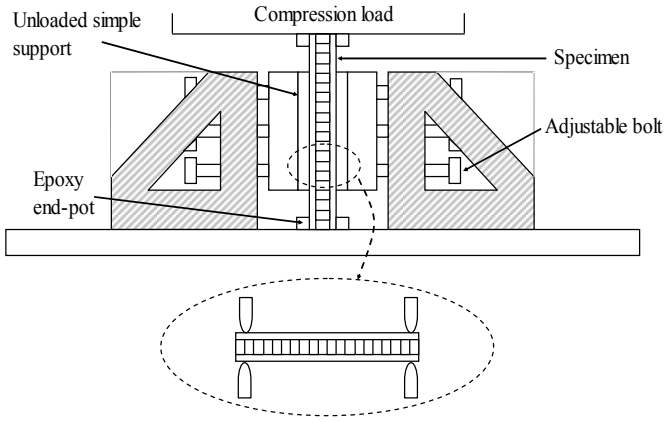

(b)

Fig. 2 (a) Specimen dimensions and strain gauge locations and (b) experimental set-up of a panel in compression with unloaded edge support rig

4 Damage Mechanisms and Energy Absorption in Sandwich Panels

The initiation and propagation characteristics of damage mechanisms in sandwich panels in bending were ascertained through extensive examination of not only impact test results but also quasi-static as well as indentation test results in addition to systematic microscopic inspections of cut cross sections in [8-9]. For aluminium sandwich panels, the initial damage occurred at about 0.51 kN (measured quasi-statically) and was a combination

of core crushing and small delaminations. As the contact area of the HS impactor increased with load with the highest contact pressure at the apex [10], delaminations were found in the shape of a cone due to a high local stress [8]. The initial damage was followed by continued core crushing and by propagation of the top-skin delaminations right up to catastrophic failure associated with top skin fracture at about 6.22 kN (quasi-statically) (or 6.38 kN measured via impact test at 21 J). A cross-sectional view of impact-damaged aluminium panel (Al 13J 2) is shown in Fig. 3.

Table 2 Summary of CAI tests

Panel ID	IKE	Failure load	RCS	RCS retention ratio	Failure location *
-	J	kN	MPa	MPa	-
Al control 1	0	92.00	270.6	0.93	LE
Al control 2	0	111.59	322.0	1.10	LE
Al 3.7J 1	2.60	71.53	207.0	0.71	MS
Al 3.7J 2	3.66	67.11	190.7	0.65	LE
Al 3.7J 3	3.62	72.94	219.0	0.75	MS
Al 5J 1	5.20	75.50	221.8	0.76	FE
Al 5J 2	5.40	67.58	195.3	0.67	MS
Al 9.5J 1	9.54	84.45	243.9	0.83	MS
Al 9.5J 2	9.51	68.32	190.3	0.65	LE
Al 13J 1	13.68	71.54	203.8	0.70	MS
Al 13J 2	13.76	73.00	215.2	0.74	MS
Al 25J 1	24.34	63.16	187.6	0.64	MS
Al 25J 2	25.54	51.00	150.4	0.51	LE
Nom con. 1	0	97.65	283.9	0.97	LE
Nom con. 2	0	102.69	293.1	1.00	LE
Nom 5J	5.13	55.87	162. 4	0.56	MS
Nom 9J	9.23	71.60	205.6	0.70	MS
Nom 16J	16.29	65.01	187.0	0.64	MS
Nom 28J	28.20	46.53	134.1	0.46	MS

* LE, MS and FE denote loaded end, mid-section and far end, respectively.

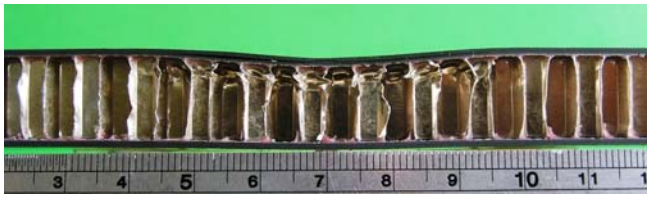

Fig. 3 An aluminium sandwich panel impacted at 13 J

In all tests, the extent of crushed core was generally greater than the extent of skin delamination. The gap between the two became greater for the given greater impact energy. The bottom skin remained intact and there was no local skin-core debonding before the ultimate load. The surface indent was also greater with the greater impact energy. The maximum depth of crushed cells at impact energy of 25 J reached about middle of the cores in both cases.

The damage characteristics of nomex panels were more or less the same as aluminium ones, though the fractured nomex cells with a lesser degree of cells folding showed substantial spring-back upon unloading. Furthermore, the initial flexural rigidity of the nomex panels (within the elastic range) was significantly lower than those of the aluminium ones due to the fact that the shear strength and modulus of the nomex cores were significantly lower. In addition, the local indentation in the nomex panels was found to be very dominant. This is interesting in considering the fact that the impacted nomex panels exhibited much less surface indent with the maximum depth of crushed cells reaching only about middle of the core height from impact of 28 J. A cross-sectional view of impact-damaged nomex panel (Nom 16J) is shown in Fig. 4.

Fig. 4 A nomex sandwich panel impacted at 16 J

Fig. 5 shows the extensions of both top skin delaminations and crushed core in terms of impact energy. The increase in the both extensions is nonlinear at the low end of energy range. The dominant middle region exhibits a steady and linear growth with an increase of impact energy. In the final region, all the extensions seemed to level off or decrease slightly after the occurrence of top skin fracture. These trends are in accordance with the energy-absorbing characteristics in Fig. 6. In the initial and middle regions, an increase in energy absorption is linear and an absorbed energy (E_{ab}) is around about 67% of impact energy. Once the top skin fracture occurred, absorbed energy is increased up to over 90%. The overall similarity in the mechanical response and energy-absorbing

characteristics between the aluminium and nomex panels suggests that their CAI data could be pooled.

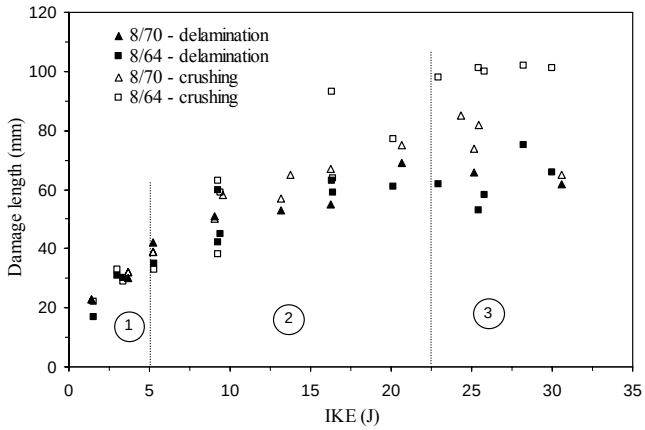

Fig. 5 Extent of delamination and crushed core in both aluminium and nomex sandwich panels

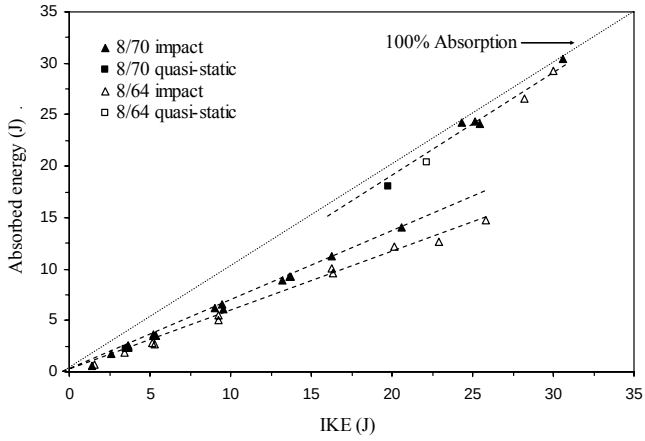

Fig. 6 Absorbed energy of aluminium and nomex honeycomb sandwich panels

5 Residual In-Plane Compressive Behaviour

5.1 In-Plane Compressive Behaviour

The in-plane compressive behaviour of the damaged sandwich panels was very complex due primarily to two factors. One is that the sandwich itself was complex structure on its own during in-plane compression because the two skins were stabilised and supported by the core to some degree. Thus, substantial part of knowledge and understanding established from the compression of monolithic panels [11-12] did not necessarily apply. The other is that, while the distal skin remained undamaged after impact, the impacted skin around the mid-section region was damaged with the core underneath being crushed. Therefore, the residual compressive performance of the damaged panels was attributed not only to the strength degradation of the compressive skin associated with the damage but also to the lack of symmetry for the panels with respect to the in-plane compression loading and supporting conditions and interaction between the skins and core in each of such panels.

All in-plane compression test results from both intact and impact-damaged panels are summarised in Table 2. The compressive behaviour of an undamaged aluminium panel (Al control 2) is shown in Fig. 7 in the both longitudinal and transverse directions. The tilting of one panel end at the early stage of loading is indicated via the bending strain response of the far-field strain gauges (SG1). As the local strain gauges (SG2) on the mid-section exhibit very small bending strain with large mean strain, these responses provide no indication of local buckling, let alone the transition of local buckling to mode II buckling. Thus the panel failed in the region which is very close to the loaded end as shown in Fig. 8. The compressive behaviour of undamaged nomex panels is very similar in terms of both strain response and failure characteristic.

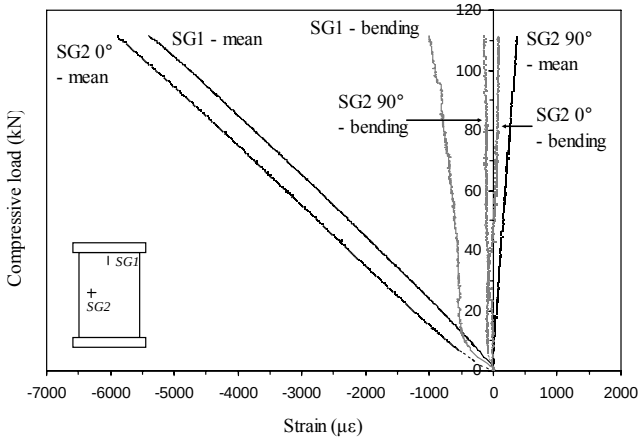

Fig. 7 Mean and bending strain responses of an undamaged aluminium sandwich panel

Once impact damage was inflicted in panels, about two thirds of the aluminium panels failed around the mid-section region, which was weakened by the presence of impact damage, as one example shows in Fig. 9. And all the impact-damaged nomex panels failed in the same way. About a third of the impacted aluminium panels (see Table 2) failed in a similar way to the control panels, that's failure close to one loaded end. Moreover, this result did not appear to be affected by the degree of impact

damage, as impact energies applied to those four respective panels spread from 3.7 J to 25 J. In the last case with impact energy of 25 J, the respective extents of delamination in the impacted skin and crushed core were close to half the panel width. A further examination of the compressive strain responses reveals that for aluminium panels there was little difference in terms of residual compressive strength (RCS) between those that failed around the mid-section region and those that did not. An example given in Fig. 10 from specimen 'Al 13J 2' that failed around mid-section shows similar strain responses to those of the undamaged panels in Fig. 7. However, the majority of the impact-damaged nomex panels did show classic strain reversal shown in Fig. 11 at about 65 kN, which immediately triggered catastrophic failure.

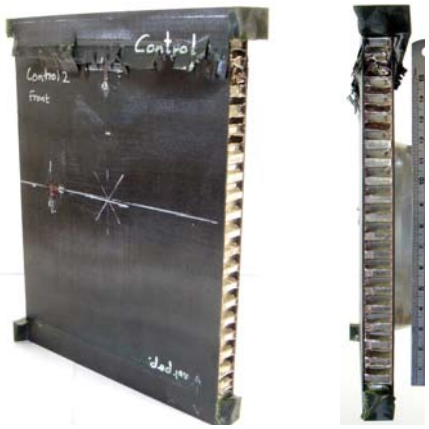

Fig. 8 Photographs of an undamaged aluminium sandwich panel after compression test

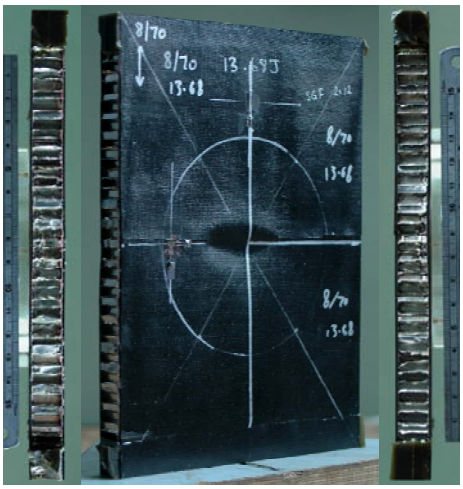

Fig. 9 Photographs of an impact-damaged aluminium sandwich panel after CAI test

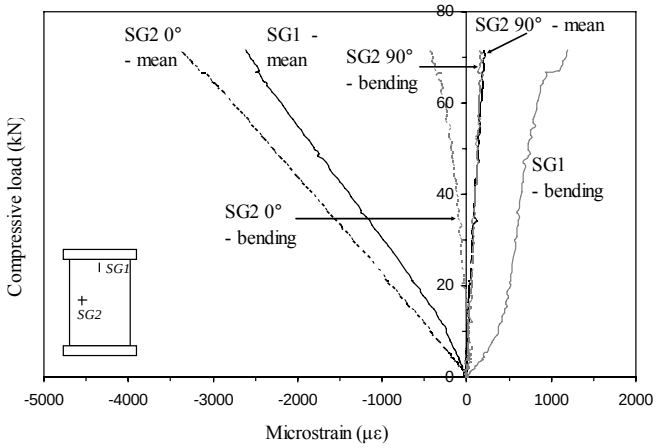

Fig. 10 Mean and bending strain responses of aluminium sandwich panel Al 13J 2 impacted at 13 J

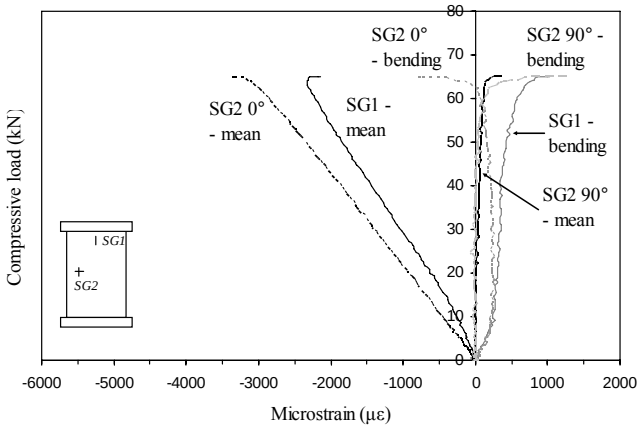

Fig. 11 Mean and bending strain responses of nomex sandwich panel Nom 16J impacted at 16 J

5.2 Contribution of Honeycomb Core

Although the impact damage tolerance philosophy for sandwich panels in the aerospace industry is adapted from that for monolithic laminated panels, the role played by the core in the in-plane compressive behaviour of sandwich panels has not been addressed. A nominal width-to-thickness ratio of a sandwich panel is generally much smaller than that of a monolithic panel as its thickness increase is much more than the increase in its length and width. In particular, the presence of the core between the two skins provides a constraint in the through-the-thickness direction to both longitudinally transverse shear and normal compression. As a result, the compressive properties of the core such as core density, transverse shear stiffness, bare compressive strength and crush strength become much more critical to the in-plane compressive behaviour of

sandwich panels. Therefore, it could be logically deduced that the denser core and/or core with greater transverse shear stiffness provides sandwich panels with much stronger compressive resistance. This appears to be the case when the aluminium panels with much greater transverse shear moduli were compared to the nomex panels.

Moreover, for both types of panels, the tensile strength of adhesive of about 5.5 MPa is substantially greater than the stabilised compressive strength of 4.2 MPa for aluminium and 4.0 for nomex. This suggests that the compressed distal skin had to crush core first or dimple rather than wrinkle outwards, whereas the impact damaged skin was in the dished shape and thus was prone to either compressing the already crushed core further (see Fig. 9) or buckling outward, as illustrated in Fig. 12. In aluminium sandwich panels, crushing was close to the distal skin. The in-plane compressive loads were not sufficient to bend the skins within the damaged region due to the high local flexural rigidity and shear rigidity. In nomex sandwich panels, the fractured cells were close to the mid-plane of the panels. These results seem to suggest that the simple support to unloaded edges somewhat shifted the in-plane compressive resistance to the outer regions where the core cells were largely undamaged. As a result, it could be deduced that for the same damage the sandwich panel with denser core could provide greater compressive strength. This seems to be confirmed by [13].

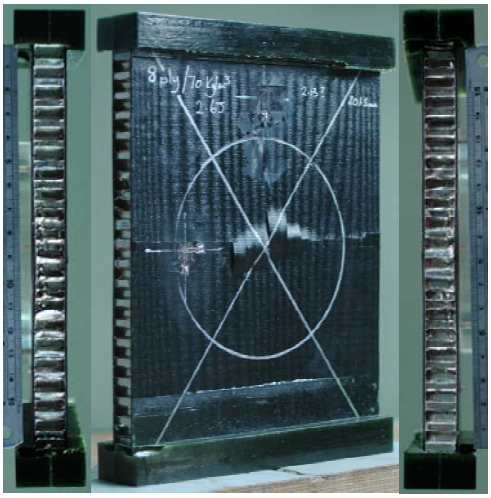

Fig. 12 Photographs of an impact-damaged aluminium sandwich panel after CAI test showing crushed core around the mid-section region

5.3 Impact Damage Tolerance

Tolerance of impact damage is assessed in Fig. 13 through residual compressive strength in terms of impact energy, which includes both aluminium and nomex panel results. A moderate reduction of compressive strength was immediate once panels were impact-damaged. From 3.7 J to 13 J, however, the variation of residual compressive strength is limited. The state of damage in these panels over this region is dominated by core crushing and skin delaminations. Although the corresponding increase of both crushed core and delamination extents is about 75% over the impact energy range, the aforementioned contribution of the core to stabilising the mid-section region reduced the likelihood of local buckling development. Therefore, the effect of impact damage was cancelled out, to some extent, by the buckling constraint contribution of the core and is manifested in this limited variation of residual compressive strength.

When impact energy level reached over 20 J, a further reduction of residual compressive strength became noticeable because of the fracture of the impacted skins. At the highest impact energy, the reduction of compressive strength was about 50% for both honeycomb sandwich panels. In addition, it is interesting to note that the different failure locations among the CAI tested panels are not distinguished over the values of residual compressive strength.

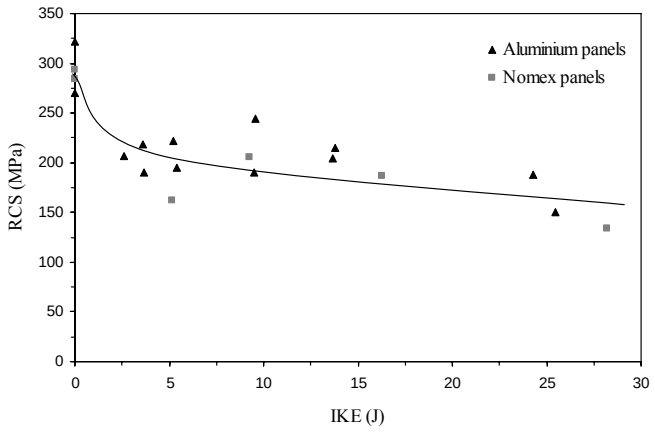

Fig. 13 Variation of residual compressive strength with IKE for sandwich panels

These results are also presented in Fig. 14 with the compressive strength retention factor plotted against damage extent. Although there is some data

variation as circled by a dashed ellipse, the 'major axis' of the ellipse seems to form a linear trend back the baseline values.

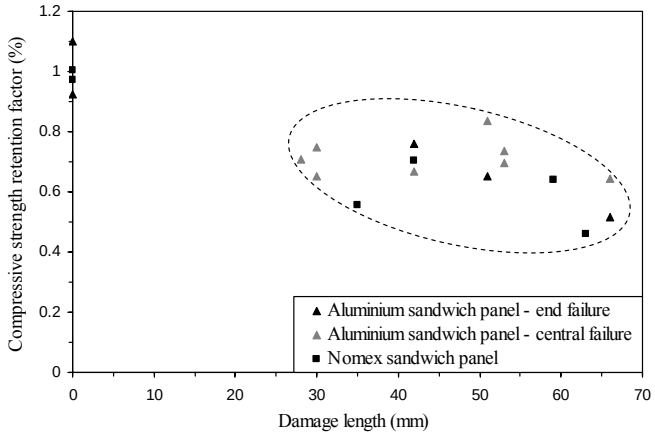

Fig. 14 Variation of compressive strength retention factor with damage length

The damage tolerance of impact-damaged panels is also assessed through residual mean compressive strains obtained from the far-field strain gauge locations in Fig. 15. Although the overall trend here is similar to that in Fig. 13, the value of strain loss seems to be slightly worse than RCS. This is also noticeable for nomex panels, though more data and further investigation in future will be needed.

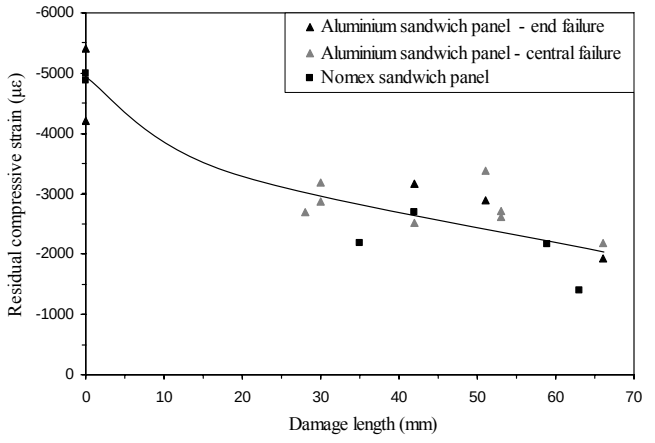

Fig. 15 Variation of residual compressive strain with damage length

6 Conclusions

Both aluminium and nomex composite sandwich panels with 8 ply carbon/epoxy skins and core density between 64 and 70 kg/m^3 were damaged by impact and quasi-static loads. Impact tests were conducted at impact energy ranging from 2 J to 55 J. Dominant damage mechanisms found were core crushing, (impacted) skin delamination and skin fracture with the former two absorbing most impact energy. The skin fracture started occurring after about 20 J in both types of panels. As the initial damage occurred at relatively low load, energy absorption up to skin fracture was completely dominant and took place locally through cell crushing. Different core materials with a similar density made little difference on either the damage or energy-absorbing characteristics.

Both intact and impact-damaged composite sandwich panels were further investigated through in-plane compression. While undamaged panels failed in region close to one loaded end due to high flexural rigidity of the panels, all impact-damaged nomex panels along with two thirds of aluminium panels failed around the mid-section region. However, one third of aluminium panels failed in the loaded end region. The presence of the core played a unique role in in-plane compression and it seemed to counteract the deleterious effect of impact damage. The in-plane compressive behaviour has generally shown combined effects of impact damage and the core in a complex manner, as RCS values did not reflect the different compression deformation characteristics.

References

[1] Abrate S. "Localized impact on sandwich structures with laminated facings", *Applied Mechanics Review*, Vol. 50, pp69-82, 1997.

[2] McGowan D.M. and Ambur D.R. "Damage characteristics and residual strength of composite sandwich panels impacted with and without a compression loading", *AIAA-98-1783*, pp713-723, 1998.

[3] Tomblin J.S., Lacy T., Smith B., Hooper S., Vizzini A. and Lee S. "Review of damage tolerance for composite sandwich airframe structures", *FAA Report, Number DOT/FAA/AR-99/49*, pp1-71, 1999.

[4] Tomblin J.S., Raju K.S., Liew J. and Smith B.L. "Impact damage characterization and damage tolerance of composite sandwich airframe structures", *DOT/FAA/AR-00/44*, pp1-181, 2001.

[5] Tomblin J.S., Raju K.S., Liew J. and Smith B.L. "Impact damage characterization and damage tolerance of composite sandwich airframe structures - Phase II", *DOT/FAA/AR-02/80*, pp1-87, 2002.

[6] Lacy T.E. and Hwang Y. "Numerical modeling of impact-damaged sandwich composites subjected to

compression-after-impact loading", *Composite Structures,* Vol. 61**,** pp115-128, 2003.

[7] Tomblin J.S., Raju K.S. and Arosteguy G. "Damage resistance and tolerance of composite sandwich panels - scaling effects", *DOT/FAA/AR-03/75*, pp1-70, 2004.

[8] Zhou G., Hill M.D. and Hookham N. "Damage characteristics of composite honeycomb sandwich panels in bending under quasi-static loading". *Journal of Sandwich Structures and Materials,* Vol. 8, pp55-90, 2006.

[9] Zhou G., Hill M.D. and Hookham N. "Investigation of parameters governing the damage and energy-absorbing characteristics of honeycomb sandwich panels", accepted by *J. of Sandwich Structures and Materials*.

[10] Zhou G. "Static behaviour and damage of thick composite laminates", *Composite Structures,* Vol. 36, pp13-22, 1996.

[11] Zhou G., and Rivera L. "Investigation for the reduction of in-plane compressive strength in preconditioned thin composite panels". *Journal of Composite Materials,* Vol. 39, pp391-422, 2005.

[12] Zhou G., and Rivera L. "Investigation for the reduction of in-plane compressive strength in preconditioned thick composite panels". *Journal of Composite Materials,* to appear.

[13] Nokkentved A., Lundsgaard-Larsen C. and Berggreen C. "Non-uniform compressive strength of debonded sandwich panels - I. Experimental investigation", *Journal of Sandwich Structures and Materials,* Vol. 7, pp461-482**,** 2005.